Process Parameter Optimization of A-TIG Welding on P22 Steel

A. R. Pavan, B. Arivazhagan and M. Vasudevan

Abstract In the present study, the Activated Tungsten Inert Gas (A-TIG) welding process parameters for welding of 2.25Cr-1Mo (P22) steel have been optimized to attain desired weld bead geometry. Before fabricating weld joints, it is essential to understand the effect of A-TIG welding process parameters in producing quality weld joints. It is proposed to employ the Response Surface Methodology (RSM) of the design of experiments (DOE) approach to determine the optimum parameters in P22 steel weld joint. First, using RSM, a design matrix will be generated by considering various input variables such as welding current, arc gap, torch velocity and electrode tip angle and the output responses such as depth of penetration (DOP), bead area and heat-affected zone (HAZ) width. Further, regression models were generated to correlate the input variables and output responses. The optimum process parameters to obtain the desired DOP, bead area and HAZ width have been determined mainly by utilizing the regression equations and the desirability approach. The Root Mean Square Error (RMSE) of the predicted and measured DOP, HAZ width, and bead area was minimum 0.2571 mm, 0.1776 mm and 6.628 mm^2, respectively. TIG current from 235 to 270 A, arc gap from 2.2 to 2.9 mm and welding speed from 60 to 75 mm/min is obtained from RSM analysis as an optimum process parameter. The study manifest that there is an excellent agreement between the predicted and measured values.

Keywords P22 steel · A-TIG welding · Depth of penetration and response surface methodology

A. R. Pavan
Homi Bhabha National Institute, Mumbai, India
e-mail: pavanar@igcar.gov.in

B. Arivazhagan · M. Vasudevan (✉)
Metallurgy and Materials Group, Indira Gandhi Centre for Atomic Research, Kalpakkam 603102, Tamil Nadu, India
e-mail: dev@igcar.gov.in

1 Introduction

During fabrication of engineering components, welding is a major joining method employed. Therefore, joining and employing the Cr–Mo ferrite steels in severe servicing conditions will affect its lifetime [1, 2]. Thus, joining is an essential method involved in the fabrication of engineering components, where welding is employed to coalesce two metals through fusion. Welding introduces very complex thermal cycle, which results in introducing residual stresses in the material [3]. This often leads to distortion, brittle fracture, and hydrogen embrittlement. This can overcome by proper choice of the welding process.

Fabrication of thicker weld joints using conventional TIG welding process requires joint (groove) preparation, filler material and needs multiple numbers of welding passes. On the other hand, A-TIG welding has enhanced the performance and productivity by threefold [4]. In this technique, the flux is prepared using fine particles of strong deoxidizers dissolved in acetone to form a paste and applied over the joint. During welding, the flux disintegrates to produce oxygen that alters the flow of the molten pool called Marangoni convection eventually to yield an increased DOP [5]. The oxygen content increases the surface tension gradient eventually this increases the depth to width ratio [5]. The A-TIG welding process helps in achieving high productivity [6], lower residual stress and distortion [7].

In the present work, the objective is to determine optimum A-TIG welding parameters to obtain the desired weld shape in P22 steel. For optimizing all independent variables such as current (A), welding speed (mm/min), and Arc gap (mm) the most widely used method is RSM. The main advantage of RSM is it mainly reduces human efforts in achieving the desired output with a minimum number of experiments.

RSM is a useful method to control the input parameters for obtaining the desired response. The output response for respective inputs is analyzed by a series of experiments by using the DOE approach. Central Composite Design (CCD) is the well-known method in RSM, which uses the properties of rotatability to determine the factors. Eventually, the optimum response can be graphically analyzed using contour plots.

Several authors have used the RSM tool to optimize the input variables. Vasantharaja et al. [8] have efficiently correlated the generated model solutions with experimental values and found the actual parameters required to join the 10 mm thick RAFM steel by using A-TIG welding. Nanda et al. [9] demonstrated the influence of the A-TIG welding parameters on the weld geometry of duplex stainless steel alloy 2205. Benyounis et al. [10] successfully demonstrated how the laser power and welding speed alters the geometry of the weld bead and also showed how to get efficient welds exhibiting good mechanical properties with optimized parameters. Ragavendran et al. [11] reported the influence of TIG current and laser power on DOP and finally arrived at a set of optimum parameters to join 5.6 mm thick type 316 LN steel plates. However, there is not much literature available on the multi-response process parameter optimization for joining of P22

steels using A-TIG welding. In the present study, we have tried to determine the best possible parameter for A-TIG welding of P22 steels eventually to attain desired DOP, HAZ width and minimum weld bead area, also called multi-response optimization. By using the design of experiments software, CCD is used to generate the design matrix for carrying out the experiments. The optimized parameters have been verified through experiments.

2 Experimental

P22 plates of dimension $300 \times 120 \times 10$ mm was used in the preparation of bead-on-plate welds. The P22 steel chemical composition is given in Table 1.

A tungsten electrode (dia.3.2 mm) with a 60° tip angle was employed to generate the arc. Argon is used to prevent the oxidation at the flow rate of 10 L/min. The generated design matrix is shown in Table 3. The three input variables were varied at five-level in CCD, with eight factorial points ($2^3 = 8$), six center points, and six-star points collectively to get 20 number of data sets as shown in Tables 2 and 3. The 20 number of small specimens were extracted from the weld plate which is polished and finally etched using 10% nitric acid dissolved in ethanol. The region of interest from weld bead geometry is analyzed using an optical microscope. The respective details are then given to the Design expert for further analysis which is presented in Table 3.

3 Results and Discussion

Significance tests are conducted by portioning the variability of a data set also referred to as analysis of variance (ANOVA). Here the main objective is to fit the model to attain the desired response; to get optimum weld bead geometry by

Table 1 P22 Steel chemical composition

Element	C	Mn	Si	Cr	Mo	Cu	Ni	P	S
Weight (%)	0.15	0.5	0.2	2.25	1	0.05	0.2	0.02	0.02

Table 2 Process parameters varied at five levels

Parameters	Unit	Level 2	Level 1	Level 0	Level 1	Level 2
Current	A	100	141.54	200	259.46	300
Arc gap	mm	1	1.41	2	2.59	3
Torch speed	mm/min	60	72.16	90	107.84	120

Table 3 Generated Design Matrix with the Experimentally Measured Responses

Run	Type	Factor 1 A: current (A)	Factor 2 B: arc gap (mm)	Factor 3 C: torch speed (mm/min)	Response 1 DOP (mm)	Response 2 HAZ width (mm)	Response 3 bead area (mm^2)
1	Axial	200	2	60	4.73	1.452	31.648
2	Axial	300	2	90	5.333	3.01	35.428
3	Fact	140.54	2.59	72.16	2.936	1.14	14.556
4	Fact	259.46	2.59	72.16	6.303	2.9	37.53
5	Center	200	2	90	4.47	1.472	23.247
6	Center	200	2	90	4.904	1.367	24.004
7	Axial	200	2	120	3.943	1.424	20.863
8	Center	200	2	90	4.892	1.567	25.371
9	Fact	140.54	1.41	107.84	4.943	1.73	18.533
10	Fact	259.46	1.41	107.84	3.587	1.621	23.5
11	Fact	140.54	2.59	107.84	2.798	1.405	13.192
12	Center	200	2	90	5.063	1.608	25.21
13	Axial	100	2	90	2.016	1.18	4.943
14	Center	200	2	90	4.987	1.52	25.171
15	Fact	140.54	1.41	72.16	3.517	1.268	20.556
16	Axial	200	1	90	4.873	1.875	29.461
17	Axial	200	3	90	4.457	2.161	25.845
18	Fact	259.46	1.41	72.16	5.322	2.25	43.711
19	Fact	259.46	2.59	107.84	4.222	2.47	28.791
20	Center	200	2	90	5.172	1.409	23.878

developing the polynomial equations between the independent variables and responses RSM is the key tool utilized.

RSM effectively utilizes the independent variables to fit the numerical model. A polynomial regression Eq. (1) is generated to demonstrate the optimum response.

$$Y = b_0 + b_1x_1 + b_2x_2 + b_3x_3 + b_4x_1^2 + b_5x_2^2 + b_6x_3^2 + b_7x_1x_2 + b_8x_1x_3 + b_9x_2x_3$$

(1)

Here, b_0 constant; b_1 to b_9 represents the coefficients. The terms X_1, X_2, X_3, X_1^2, X_2^2, X_3^2, X_1X_2, X_1X_3 and X_2X_3 correspond to the process parameters. Previously in some of literatures reported, similar analysis procedure was carried out [8].

ANOVA determines the significance level of the process parameters and its interaction level. The adjusted R-squared value decides the fitness of the model. The model is adequate when the adjusted R-squared is nearly equal to one. The Model F-value of 24.47, 62.69, and 66.18 for DOP, HAZ width and weld bead area, respectively suggests the significance of the model. The model terms are significant

Table 4 ANOVA for DOP

Source	Sum of squares	df	Mean square	F value	p-value Prob > F	
Model	19.05	9	2.12	24.47	<0.0001	Significant
A-current	8.57	1	8.57	99.08	<0.0001	
B-arc gap	0.24	1	0.24	2.77	0.1269	
C-torch speed	1.09	1	1.09	12.56	0.0053	
AB	2.36	1	2.36	27.25	2.36	
AC	3.26	1	3.26	37.65	3.26	
BC	0.46	1	0.46	5.27	0.46	
A2	2.72	1	2.72	31.42	2.72	
B2	0.10	1	0.10	1.18	0.10	
C2	0.58	1	0.58	6.68	0.58	
Residual	0.86	10	0.086			
Lack of fit	0.57	5	0.11	1.96	0.2383	Not significant
Pure error	0.29	5	0.058			
Cor total	19.92	19				

R-Squared- 0.9566; Adj R-Squared 0.9175; Pred R-Squared 0.7457; Adeq Precision 20.211

only when the "Prob > F" value is less than 0.050. ANOVA analysis for the DOP, HAZ width and weld bead area responses are shown in Tables 4, 5 and 6.

The value of Adeq Precision estimates the signal to noise ratio, and the value of Adeq Precision greater than 4 is advisable. Moreover, in this model, for DOP, HAZ width and weld bead area are 20.211. 27.669, and 33.251, respectively, indicate the adequacy of the signal in the model. The regression equation derived by using all input variables such as Current (A), Arc gap (B), and Torch speed (C) that represents the response surface is given as follows:

$$DOP = +4.91 + 0.79 \times A - 0.13 \times B - 0.28 \times C + 0.54 \times A \times B - 0.64 \times A \times C$$
$$- 0.24 \times B \times C - 0.43 \times A^2 - 0.084 \times B^2 - 0.20 \times C^2$$

(2)

$$HAZ\,Width = +1.49 + 0.50 \times A + 0.11 \times B - 0.028 \times C + 0.24 \times A \times B - 0.22 \times A \times C$$
$$+ 2.5E - 004 \times B \times C + 0.21 \times A^2 + 0.18 \times B^2 - 0.024 \times C^2$$

(3)

$$Bead\,Area = +24.47 + 8.64 \times A - 1.34 \times B - 3.70 \times C + 1.31 \times A \times B - 3.20 \times A \times C$$
$$+ 1.52 \times B \times C - 1.45 \times A^2 + 1.19 \times B + 0.70 \times C^2$$

(4)

Table 5 ANOVA for HAZ width

Source	Sum of squares	df	Mean square	F value	p-value Prob > F	
Model	5.47	9	0.61	62.69	<0.0001	Significant
A-current	3.36	1	3.36	346.62	<0.0001	
B-arc gap	0.17	1	0.17	17.60	0.0018	
C-torch speed	0.011	1	0.011	1.08	0.3221	
AB	0.48	1	0.48	49.11	0.48	
AC	0.40	1	0.40	41.11	0.40	
BC	5.0E-7	1	5.0E-007	5.16E-5	5.0E-7	
A^2	0.63	1	0.63	64.67	0.63	
B^2	0.47	1	0.47	48.90	0.47	
C^2	8.07E-3	1	8.07E-3	0.83	8.07E-3	
Residual	0.097	10	9.70E-3			
Lack of fit	0.054	5	0.011	1.27	0.4004	Not significant
Pure error	0.043	5	8.55E-3			
Cor total	5.57	19				

R-Squared- 0.95826; Adj R-Squared 0.9669; Pred R-Squared 0.9095; Adeq Precision 27.669

Table 6 ANOVA for bead area

Source	Sum of squares	df	Mean square	F value	p-value Prob > F	
Model	1407.62	9	156.40	66.18	<0.0001	Significant
A-current	1018.95	1	1018.95	431.17	<0.0001	
B-arc Gap	24.55	1	24.55	10.39	0.0091	
C-torch Speed	186.55	1	186.55	78.94	<0.0001	
AB	13.65	1	13.65	5.78	13.65	
AC	81.68	1	81.68	34.56	81.68	
BC	18.40	1	18.40	7.78	18.40	
A^2	30.20	1	30.20	12.78	30.20	
B^2	20.49	1	20.49	8.67	20.49	
C^2	7.03	1	7.03	2.97	7.03	
Residual	23.63	10	2.36			
Lack of fit	19.72	5	3.94	5.04	0.0502	Not significant
Pure error	3.91	5	0.78			
Cor total	1431.25	19				

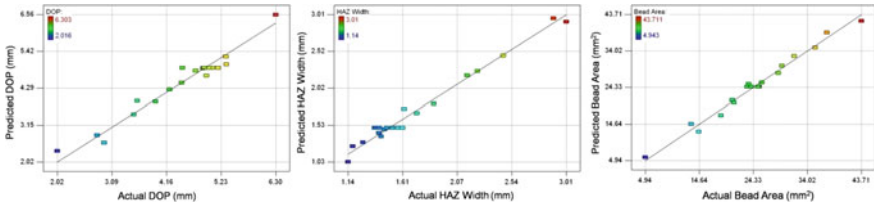R-Squared- 0.9835, Adj R-Squared 0.91686, Pred R-Squared 0.8754, Adeq Precision 33.251

Fig. 1 Predicted versus actual responses

The above equations (Eqs. (2), (3) and (4)) will be used in the desirability analysis to achieve the optimum result. The predicted versus actual value of the obtained response variable is depicted in Fig. 1. Actual values show good agreement with the predicted model values. Here, current (A), Arc gap (B), and Torch speed (C) and the interaction factors of AB, AC, BC, A^2, B^2, and C^2 are recommended to be the significant model terms.

3.1 Interaction of Input Variables on DOP

From ANOVA, the input variables and its interaction showed prominent effects on the output. The effect of the parameter on the outcome can be determined by the generated models. Process parameters, interaction effects can be examined by keeping the third parameter at the central level. The interactions between current, arc gap and torch speed on DOP are presented in Fig. 1, which is derived from the mathematical model shown in Eq. (1). The interaction plots between the input variables suggest that DOP is mainly controlled by current, which is clear from the ANOVA Table 4. With an increase in welding current (100–300 A) DOP increases. Similarly, the DOP increases with the decrease in welding speed (120–60 mm/min) due to a decrease in supplied heat input. Lower welding speed and high current results higher DOP. Also, it can be noted that the influence of current is more to increase DOP compared to all other parameters which can be seen in Table 4 (Fig. 2).

3.2 Interaction of Input Variables on HAZ Width

The interaction of current, torch speed, and arc gap on HAZ width are shown in Fig. 3a. It is evident from the figure that, as the current increases HAZ width increases. HAZ width depends on the TIG current and welding speed. At higher current and lower speed, HAZ width is more. As the speed increases from a certain
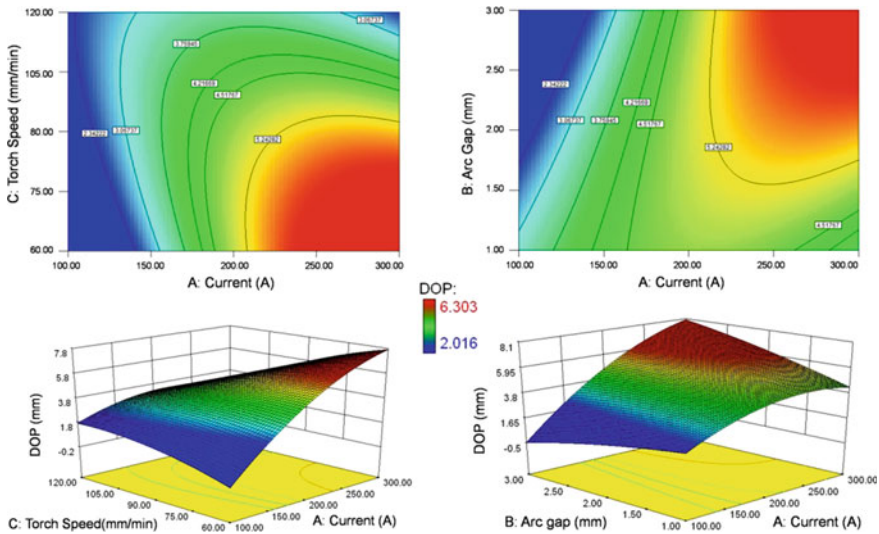
Fig. 2 Interaction between current, arc gap, and torch speed on DOP

limit (>90 mm/min), the HAZ width drastically decreases. This apparently indicates that heat flow into the base material depends on both current and torch speed. Also, it can be noted that as the arc gap increases the HAZ width increases due to the rise in heat input.

3.3 Interaction of Input Variables on Bead Area

TIG current monitors the bead area. When current is at a lower level, the obtained bead width is small, which lead to a decrease in, weld cross-sectional area. As current increases depth to width ratio increases which lead to increased weld bead area. However, higher TIG current and lower welding speed lead to maximum weld cross-sectional area (Fig. 3b).

Optimization of process parameter uses numerical and graphical approach by choosing the target for all process variables and output. Numerical approach couples all necessary targets to get a desirable response. In graphical technique optimization with varying responses, the software interprets the region with the help of a CCD model. Where the defined region gives the range of optimized parameter and the shaded regions on the overlay plot meet the proposed criteria.

For joining the thick sections of P22 steel using A-TIG welding, the primary objective is to achieve maximum DOP, targeted HAZ width and to get minimum
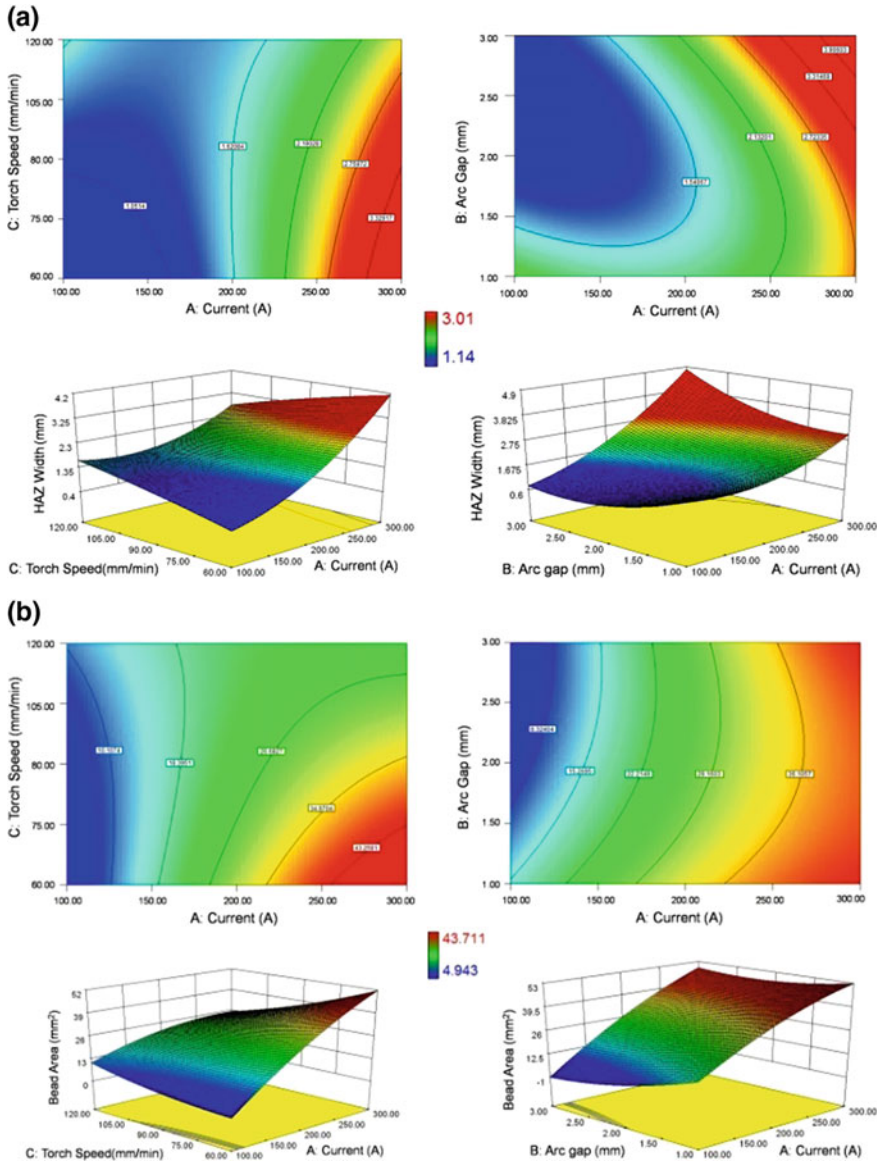
Fig. 3 The interaction between current, arc gap, and torch speed. **a** HAZ width, **b** bead area

bead area in other words, high depth to width ratio. In order to achieve targeted and the optimum result, the multi-objective optimization is necessary. Achieving full DOP during welding of thicker (10–12 mm) materials is necessary to improve the weld metal properties; hence the goal is set as maximizing the DOP, whereas the HAZ width and bead area was kept in range. Several numbers of solutions were

Table 7 Multi-response optimization criteria

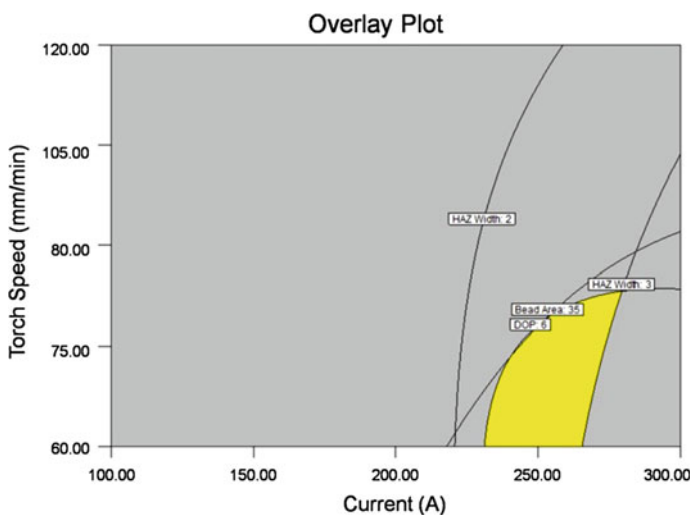| Constraints						
Name	Goal	Lower limit	Upper limit	Lower weight	Upper weight	Importance
Current	Is in range	200	300	1	1	5
Arc gap	Is in range	1	3	1	1	5
Torch speed	Is in range	60	100	1	1	5
DOP	Maximize	2.016	6.303	1	1	5
HAZ width	Is in range	1	3	1	1	5
Bead area	Is in range	4	45	1	1	5

Fig. 4 The overlay plot shows the optimum welding process parameters

produced depending on the target as shown in Table 7. RSM determined 37 solutions with respect to all three process parameters (input variables) to obtain maximum DOP and keeping the values of responses HAZ width, bead area in-range. Also, for easy understanding, graphically, the optimized results were displayed as overlay contour plots. The colored region on the contour plot (Fig. 4) meets the proposed desired criteria.

Table 8 Validation of predicted values

Sl. N0.	Current (A)	Arc gap (mm)	Torch speed (mm/min)	DOP (mm)		HAZ (mm)		Bead area (mm^2)	
				Pred.	Exp.	Pred.	Exp.	Pred.	Exp.
1	262.29	2.38	60.58	6.785	6.440	2.915	3.21	44.350	48.22
2	246.84	2.77	63.40	6.695	6.569	2.959	3.10	39.862	47.74
3	234.99	2.89	60.02	6.464	6.234	2.850	2.83	38.399	41.32
4	270.67	2.18	71.94	6.311	6.034	2.786	2.91	40.701	48.22
Root Mean Square Error (RMSE)				0.2571		0.1776		6.628	

3.4 Validation of the Model

The objective of this work is to achieve maximum DOP; hence, the predicted optimum solutions, determined by the model are validated by carrying out the experiments. Randomly, five sets of parameters are taken from the determined solutions for performing the validation experiments as shown in Table 8. The experimentally obtained actual DOP, HAZ width, and bead area values are presented in Table 8 and was found to be in good agreement with the predicted values.

4 Conclusion

The RMSE of the predicted and measured DOP, HAZ width, and bead area was very less. Hence, RSM successfully optimized the A-TIG welding process parameters for attaining the desired weld geometry. It has been found that TIG current has a major effect on the output responses compared to that of other input variables. TIG current from 235 to 270 A, arc gap from 2.2 to 2.9 mm and welding speed from 60 to 75 mm/min is obtained from RSM as an optimum process parameter. The predicted value is successfully confirmed by performing bead-on-plate experiments. The predicted result showed reasonable agreement with the experimentally measured values.

Annexure

Table 9 presents the data resulting from an investigation into the effect of three variables current (A), arc gap (B) and torch speed (C) with the respective response depth of penetration (DOP) (y). To improve the optimization process design of experiment was chosen. At first, numbers of experiments were defined based on the most important variables. The quadratic model was used to fit the result to current, arc gap and temperature.

Table 9 Experimental design matrix for response DOP with natural and coded variables

Run	Type	A			B			
		Factor 1 A: current (A)	Factor 2 B: arc gap (mm)	Factor 3 C: torch speed (mm/ min)	x_1	x_2	x_3	y Response DOP (mm)
1	Axial	200	2	60	0	0	−1.681	4.73
2	Axial	300	2	90	1.681	0	0	5.333
3	Fact	140.54	2.59	72.16	−1	1	−1	2.936
4	Fact	259.46	2.59	72.16	1	1	−1	6.303
5	Center	200	2	90	0	0	0	4.47
6	Center	200	2	90	0	0	0	4.904
7	Axial	200	2	120	0	0	1.681	3.943
8	Center	200	2	90	0	0	0	4.892
9	Fact	140.54	1.41	107.84	−1	−1	1	4.943
10	Fact	259.46	1.41	107.84	1	−1	1	3.587
11	Fact	140.54	2.59	107.84	−1	1	1	2.798
12	Center	200	2	90	0	0	0	5.063
13	Axial	100	2	90	−1.681	0	0	2.016
14	Center	200	2	90	0	0	0	4.987
15	Fact	140.54	1.41	72.16	−1	−1	−1	3.517
16	Axial	200	1	90	0	−1.681	0	4.873
17	Axial	200	3	90	0	1.681	0	4.457
18	Fact	259.46	1.41	72.16	1	−1	−1	5.322
19	Fact	259.46	2.59	107.84	1	1	1	4.222
20	Center	200	2	90	0	0	0	5.172

Levels used for A, B and C are shown in Table 1, panel A (natural variables). Panel B shows the levels in terms of coded variables x_1, x_2 and x_3

Quadratic equation for this model is shown in Eq. 5

$$Y = b_0 + b_1x_1 + b_2x_2 + b_3x_3 + b_4x_1^2 + b_5x_2^2 + b_6x_3^2 + b_7x_1x_2 + b_8x_1x_3 + b_9x_2x_3$$

(5)

This optimization process is performed using central composite design (CCD), and it is most widely used for fitting a second-order response surface. The CCD consists of 8 runs at the corners of a square, 6 axial runs and 6 runs at the center of the square and overall 20 runs. In terms of the coded variables the corners of the square are (x_1, x_2, x_3) = (−1, −1, −1), (−1, 1, −1), (1, 1, −1), (−1, −1, 1), (1, −1, 1), (−1, 1, 1), (1, −1, −1) and (1, 1, 1); the axial runs are at (x_1, x_2, x_3) = (0, 0, −1.681), (1.681, 0, 0), (0, 0, 1.681), (−1.681, 0, 0), (0, −1.681, 0) and (0, 1.681, 0) the center points are at (x_1, x_2, x_3) = (0, 0, 0). The second-order model can be fitted using the coded variables.

The coefficients of b_0 to b_9 can be estimated by using the methods of least squares, $\mathbf{b = (X^1X)^{-1}X^1y}$

For a second-order model with 20 sets of the experiment, the matrix of independent variables X and y vector for this data is

$$
X =
\begin{pmatrix}
 & x_1 & x_2 & x_3 & x_1^2 & x_2^2 & x_3^2 & x_1x_2 & x_1x_3 & x_2x_3 \\
1 & 0 & 0 & -1.681 & 0 & 0 & 2.828 & 0 & 0 & 0 \\
1 & -1.681 & 0 & 0 & 2.828 & 0 & 0 & 0 & 0 & 0 \\
1 & -1 & 1 & -1 & 1 & 1 & 1 & -1 & 1 & -1 \\
1 & 1 & 1 & -1 & 1 & 1 & 1 & 1 & -1 & -1 \\
1 & 0 & 0 & 0 & 0 & 0 & 0 & 0 & 0 & 0 \\
1 & 0 & 0 & 0 & 0 & 0 & 0 & 0 & 0 & 0 \\
1 & 0 & 0 & 1.681 & 0 & 0 & 2.828 & 0 & 0 & 0 \\
1 & 0 & 0 & 0 & 0 & 0 & 0 & 0 & 0 & 0 \\
1 & -1 & -1 & 1 & 1 & 1 & 1 & 1 & -1 & -1 \\
1 & 1 & -1 & 1 & 1 & 1 & 1 & -1 & 1 & -1 \\
1 & -1 & 1 & 1 & 1 & 1 & 1 & -1 & -1 & 1 \\
1 & 0 & 0 & 0 & 0 & 0 & 0 & 0 & 0 & 0 \\
1 & -1.681 & 0 & 0 & 2.828 & 0 & 0 & 0 & 0 & 0 \\
1 & 0 & 0 & 0 & 0 & 0 & 0 & 0 & 0 & 0 \\
1 & -1 & -1 & -1 & 1 & 1 & 1 & 1 & 1 & 1 \\
1 & 0 & -1.681 & 0 & 0 & 2.828 & 0 & 0 & 0 & 0 \\
1 & 0 & -1.681 & 0 & 0 & 2.828 & 0 & 0 & 0 & 0 \\
1 & 1 & -1 & -1 & 1 & 1 & 1 & -1 & -1 & 1 \\
1 & 1 & 1 & 1 & 1 & 1 & 1 & 1 & 1 & 1 \\
1 & 0 & 0 & 0 & 0 & 0 & 0 & 0 & 0 & 0 \\
\end{pmatrix}
\quad
Y =
\begin{pmatrix}
4.72 \\ 5.333 \\ 2.936 \\ 6.303 \\ 4.47 \\ 4.904 \\ 3.943 \\ 4.892 \\ 4.943 \\ 3.587 \\ 2.798 \\ 5.063 \\ 2.016 \\ 4.987 \\ 3.517 \\ 4.873 \\ 4.457 \\ 5.322 \\ 4.222 \\ 5.172
\end{pmatrix}
$$

And From, $b = (X^1X)^{-1}X^1y$

$$
X^1.X =
\begin{pmatrix}
20 & 0 & 0 & 0 & 13.657 & 13.657 & 13.657 & 0 \\
0 & 13.657 & 0 & 0 & 0 & 0 & 0 & 0 \\
0 & 0 & 13.657 & 0 & 0 & 0 & 0 & 0 \\
0 & 0 & 0 & 13.657 & 0 & 0 & 0 & 0 \\
13.657 & 0 & 0 & 0 & 24 & 8 & 8 & 0 \\
13.657 & 0 & 0 & 0 & 8 & 24 & 8 & 0 \\
13.657 & 0 & 0 & 0 & 8 & 8 & 24 & 0 \\
0 & 0 & 0 & 0 & 0 & 0 & 0 & 8 \\
0 & 0 & 0 & 0 & 0 & 0 & 0 & 0 \\
0 & 0 & 0 & 0 & 0 & 0 & 0 & 0 \\
\end{pmatrix}
$$

$$
X^1.y =
\begin{pmatrix}
88.46 \\ 10.81 \\ -1.80 \\ -3.85 \\ 54.41 \\ 60.01 \\ 58.15 \\ 4.34 \\ -5.10 \\ -1.91
\end{pmatrix}
\quad
b =
\begin{pmatrix}
4.91 \\ 0.79 \\ -0.13 \\ -0.28 \\ -0.43 \\ -0.08 \\ -0.20 \\ -0.54 \\ -0.63 \\ -0.23
\end{pmatrix}
$$

Therefore, the Eq. 5 can be written as shown below,

y = 4.91 + 0.79x$_1$−0.13x$_2$−0.28x$_3$ + 0.54x$_1$x$_2$−0.63x$_1$x$_3$−0.23x$_2$x$_3$−0.43x$_1^2$ −0.08x$_2^2$−0.20x$_3^2$

In terms of natural variables, the model is

y = 4.91 + 0.79A−0.13B−0.28C + 0.54AB−0.64AC−0.24BC −0.43A^2−0.08B^2−0.20C^2

Steps involved in the analysis of variance (ANOVA)

The sequence of steps involved in doing analysis of variance (ANOVA) is explained below. The ANOVA for different responses are shown in Table 4, 5 and 6 which contains the output of Design Expert. Generally, computer software will be used to fit a response surface model and to construct the contour plots. ANOVA for the selected quadratic model is an overall summary for the full model with all interactions and main effects.

Step 1: computing the sum of squares

The model sum of squares is

$$SS_{model} = SS_A + SS_B + SS_C + SS_{AB} + SS_{AC} + SS_{BC} + SS_A^2 + SS_B^2 + SS_C^2$$

$$SS_{total} = \sum (X - X^1)^2$$

$$SS_{residual} = SS_{total} - SS_{model}$$

X—Response, X^1—average of X.

Step 2: computing the degrees of freedom (DF)

$$DF = N-1$$

N is a number of observations.

Step 3: computing the mean squares (MS)

$$MS = SS/DF$$

$F = MS_{model}/MS_{residual}$

The F ratio is the ratio of two mean square values. If the null hypothesis is true, then F will have a value close to 1.0. The P value is computed from the F ratio which is computed from the ANOVA table. For each ANOVA table, various R^2 value is presented

$$R^2 = SS_{model}/SS_{total}, R_{adj}^2$$
$$= (SS_{residal}/DF_{residual})/(SS_{total}/DF_{total}) \text{ and } R_{pred}^2 1-PRESS/SS_{total}$$

PRESS = prediction error sum of squares

Step 4: a significance test

After, all the above steps are completed, the results provided in table format.

References

1. R.C. Reed, H.K.D.H. Bhadeshia, A simple model for multipass steel welds. Acta Metall. Mater. **42**, 3663–3678 (1994)
2. A. Al-Mazrouee, R.K.S. Raman, R.N. Ibrahim, Effect of post weld heat treatment on the oxide scaling of Cr–Mo steel weldments. J. Mater. Process. Technol. **164**, 964–970 (2005)
3. H. Singh, A. Singh, G.A. Singh, *Review on Residual Stress Analysis of Thick Wall Welded Pressure Vessel*, vol. 2 (2013), pp. 1–7
4. B. Arivazhagan, M. Vasudevan, Studies on A-TIG welding of 2.25Cr-1Mo (P22) steel. J. Manuf. Process. **18**, 55–59 (2015)
5. A. Berthier, P. Paillard, M. Carin, F. Valensi, S. Pellerin, TIG and A-TIG welding experimental investigations and comparison to simulation. Sci. Technol. Weld. Join. **17**, 609–615 (2012)
6. M. Vasudevan, A.K. Bhaduri, B. Raj, K.P. Rao, Genetic-algorithm-based computational models for optimizing the process parameters of A-TIG welding to achieve target bead geometry in type 304 L(N) and 316 L(N) stainless steels. Mater. Manuf. Process. **22**, 641–649 (2007)
7. V. Maduraimuthu, M. Vasudevan, V. Muthupandi, A.K. Bhaduri, T. Jayakumar, Effect of activated flux on the microstructure, mechanical properties, and residual stresses of modified 9Cr-1Mo steel weld joints. Metall. Mater. Trans. B **43**, 123–132 (2012)
8. P. Vasantharaja, M. Vasudevan, Optimization of A-TIG welding process parameters for RAFM steel using response surface methodology. *Proc. Inst. Mech. Eng., Part L: J. Mater.: Des. Appl.* **0**, 1–16 (2016)
9. N.N. Korra, M. Vasudevan, K. Balasubramanian, Optimization of A-TIG welding of duplex stainless steel alloy 2205 based on response surface methodology and experimental validation. *Proc. Inst. Mech. Eng., Part L: J. Mater.: Des. Appl.* **0**, 1–10 (2015)
10. K.Y. Benyounis, A.G. Olabi, M. Hashmi, Multi-response optimization of CO_2 laser-welding process of austenitic stainless steel. *Opt. Laser Technol.* **40**, 76–87 (2008)
11. M. Ragavendran et al., Optimization of hybrid laser–TIG welding of 316LN steel using response surface methodology (RSM). Opt. Lasers Eng. **94**, 27–36 (2017)